Electron heating in helicity-barrier-mediated turbulence

T. Adkins[1,2], R. Meyrand[2], and J. Squire[2]

[1]Princeton Plasma Physics Laboratory,
Princeton, NJ, 08540, US

[2]Department of Physics, University of Otago,
Dunedin, 9016, NZ

PPPL Theory Seminar, 12/12/24

PPPL

UNIVERSITY of OTAGO
Te Whare Wānanga o Otāgo
NEW ZEALAND
SAPERE AUDE

NeSI
New Zealand eScience Infrastructure

Large-scale motions

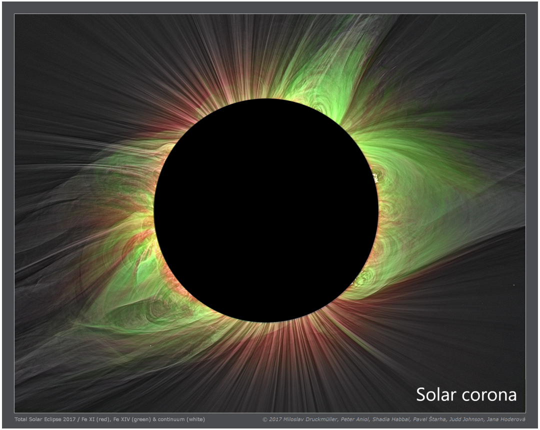

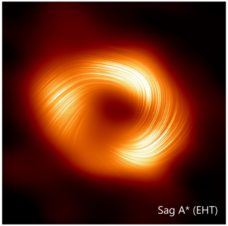

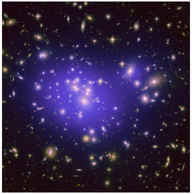

- Many astrophysical plasma systems have significant energy content in large-scale motions on scales comparable to the size of the system $\sim L$.
- <u>Problem</u>: since such motions do not dissipate, how is this energy thermalised?

Large-scale motions

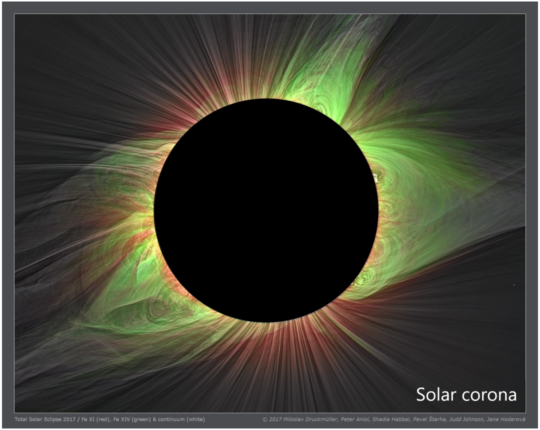

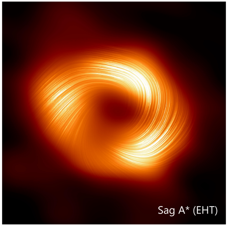

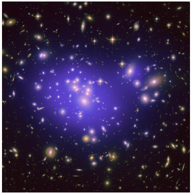

- Many astrophysical plasma systems have significant energy content in large-scale motions on scales comparable to the size of the system $\sim L$.
- Problem: since such motions do not dissipate, how is this energy thermalised?
- An answer: **turbulent heating!**

Turbulent cascade [à la Kolmogorov (1941)]

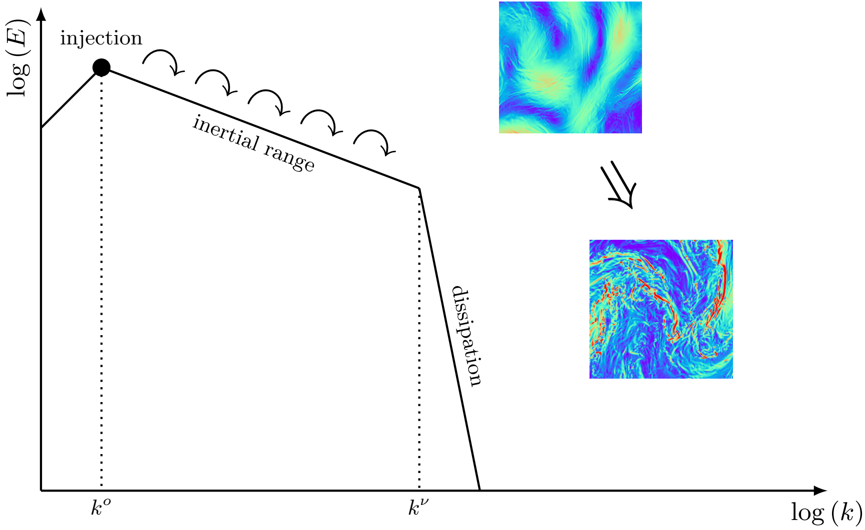

Weakly collisional plasmas

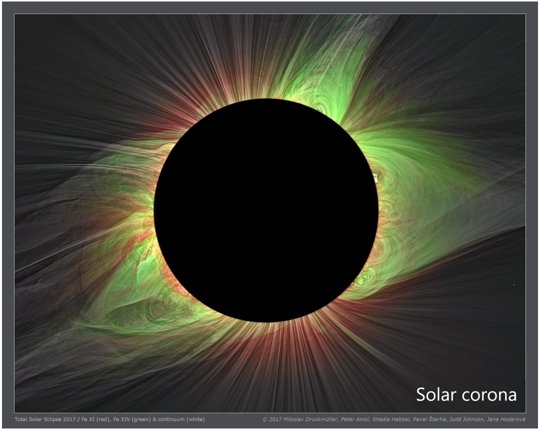

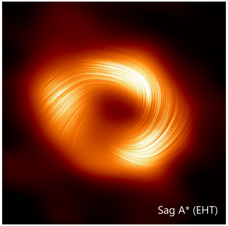

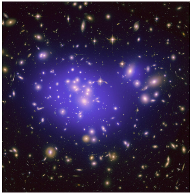

- Such plasmas are often *weakly collisional*, having characteristic dynamical timescales approaching those of the inter-particle collisions.

$$\frac{\lambda_{\text{mfp}}}{\rho_i} \sim 10^6 \left(\frac{B}{\mu\text{G}}\right) \left(\frac{T}{10^6\ \text{K}}\right)^{3/2} \left(\frac{n}{1\ \text{cm}^{-3}}\right)^{-1}.$$

Weakly collisional plasmas

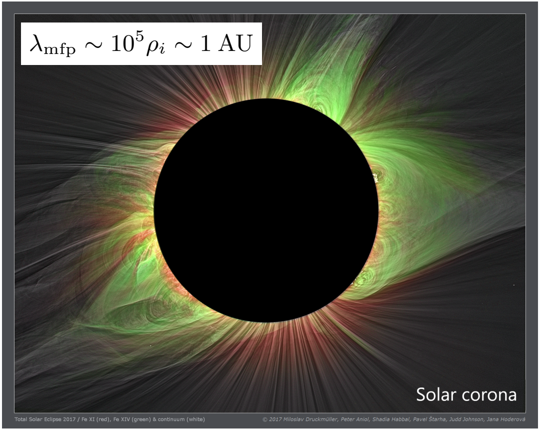

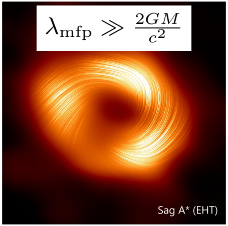

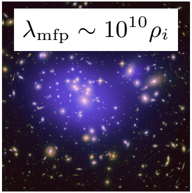

- Such plasmas are often *weakly collisional*, having characteristic dynamical timescales approaching those of the inter-particle collisions.

$$\frac{\lambda_{\rm mfp}}{\rho_i} \sim 10^6 \left(\frac{B}{\mu{\rm G}}\right) \left(\frac{T}{10^6~{\rm K}}\right)^{3/2} \left(\frac{n}{1~{\rm cm}^{-3}}\right)^{-1}.$$

Turbulent cascade (weakly collisional plasmas)

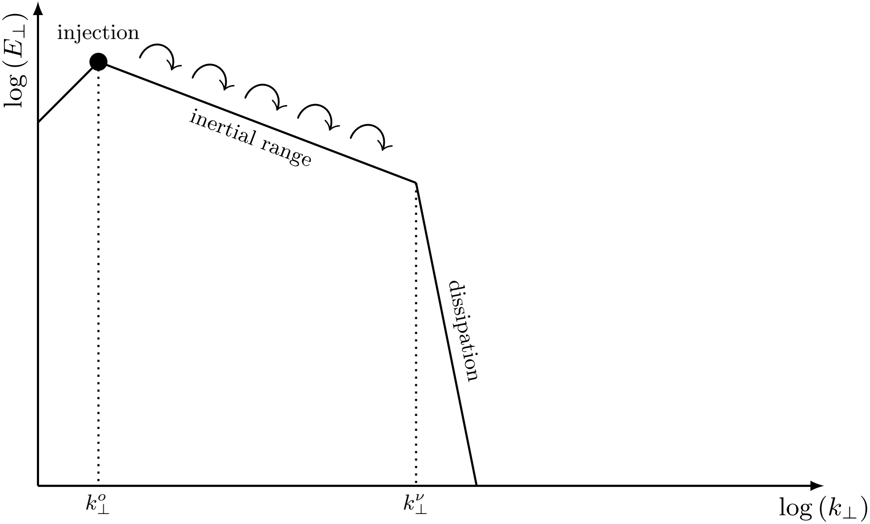

Turbulent cascade (weakly collisional plasmas)

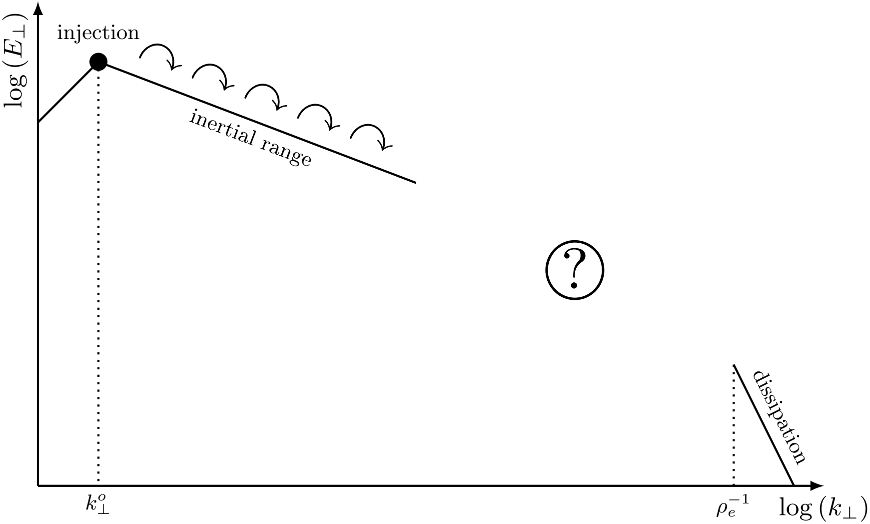

Turbulent cascade (weakly collisional plasmas)

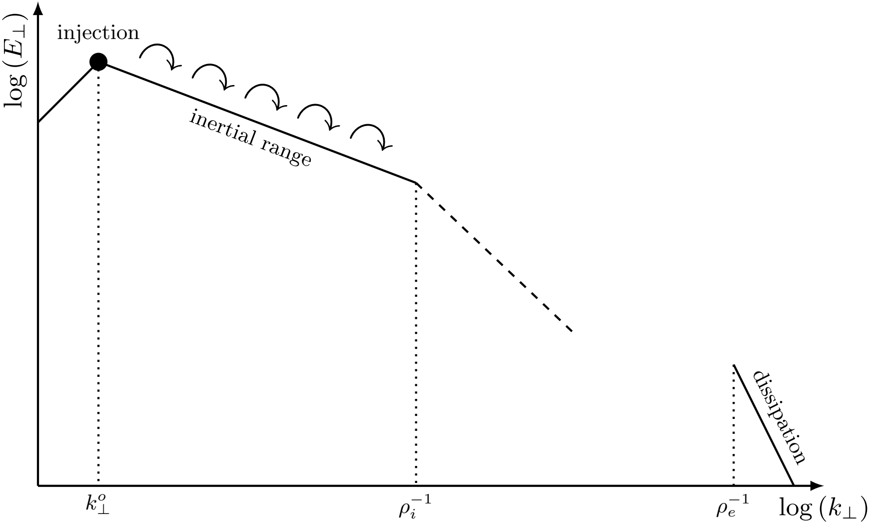

Turbulent cascade (weakly collisional plasmas)

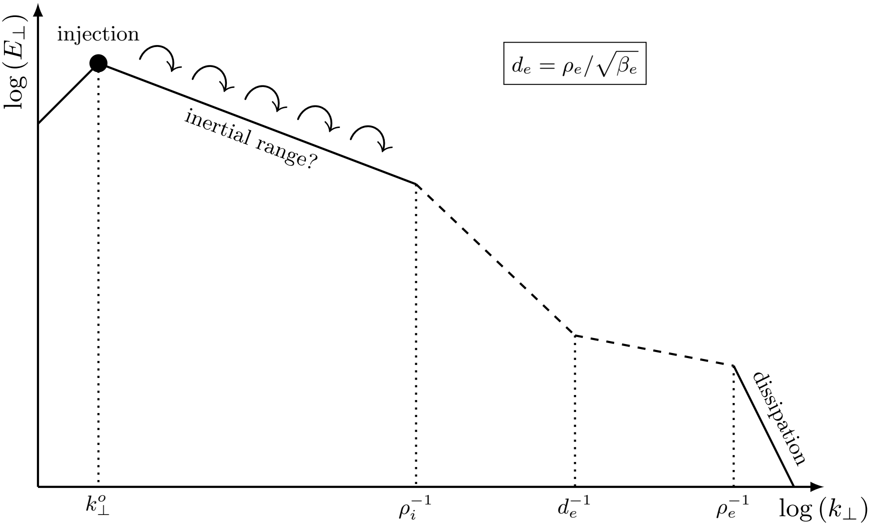

Turbulent cascade (weakly collisional plasmas)

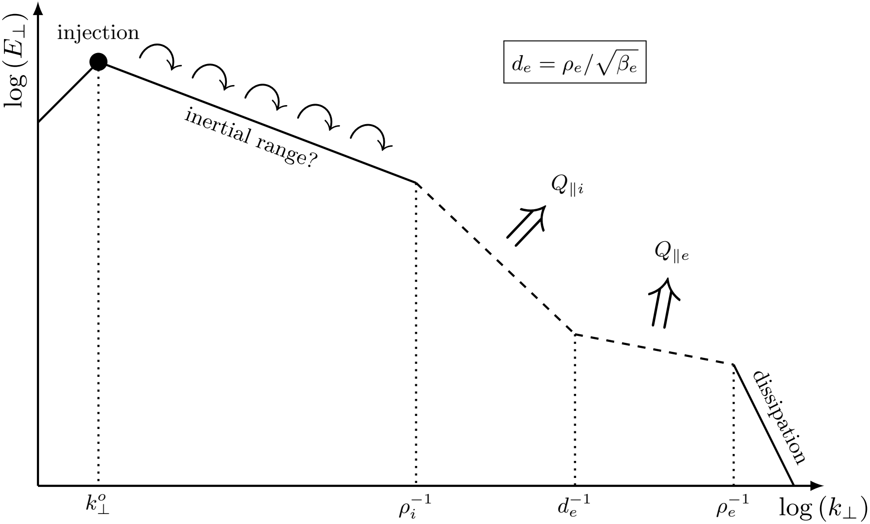

Turbulent cascade (weakly collisional plasmas)

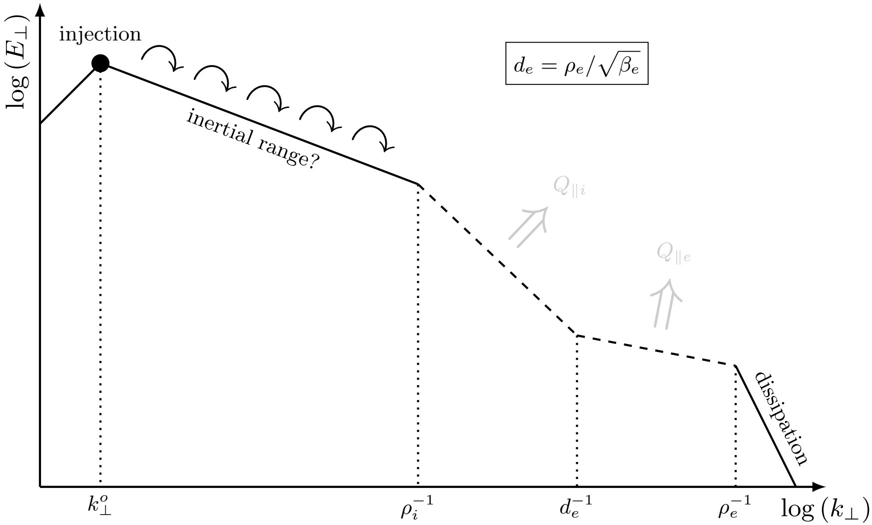

Some foreshadowing...

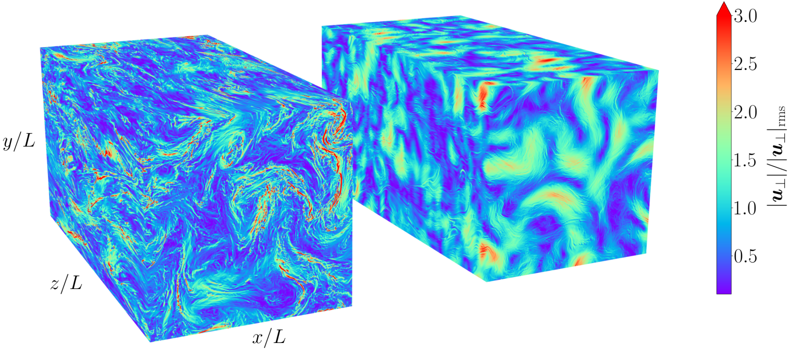

- The turbulence, and resultant heating, is **fundamentally different** depending on the value of β_e. Above shows two otherwise identical simulations with $d_e = \rho_i$ (left) and $d_e = \rho_i/2$ (right).
- A direct consequence of the role of **finite electron inertia** on the **helicity barrier** (see also Meyrand et al., 2021; Squire et al., 2022, 2023, for more on the helicity barrier).

Model equations

- Anisotropy of fluctuations $k_\parallel \ll k_\perp$ appears to be well-satisfied at small scales in the solar wind (Chen et al., 2013; Chen, 2016) $\Rightarrow$ gyrokinetics

Model equations

- Anisotropy of fluctuations $k_\parallel \ll k_\perp$ appears to be well-satisfied at small scales in the solar wind (Chen et al., 2013; Chen, 2016) $\Rightarrow$ gyrokinetics
- Two more simplifications:
  1. $\beta_e \lesssim 1$: Kinetic Reduced Electron Heating Model (KREHM)
  2. Ignore electron kinetics: isothermal KREHM

Model equations

- Anisotropy of fluctuations $k_\parallel \ll k_\perp$ appears to be well-satisfied at small scales in the solar wind (Chen et al., 2013; Chen, 2016) $\Rightarrow$ gyrokinetics
- Two more simplifications:
  1. $\beta_e \lesssim 1$: Kinetic Reduced Electron Heating Model (KREHM)
  2. Ignore electron kinetics: isothermal KREHM
- Closed fluid system:

$$\frac{\mathrm{d}\delta n_e}{\mathrm{d}t} + n_{0e}\boldsymbol{\nabla}_\parallel u_{\parallel e} = 0,$$

$$m_e n_{0e}\frac{\mathrm{d}u_{\parallel e}}{\mathrm{d}t} + T_{0e}\boldsymbol{\nabla}_\parallel \delta n_e = -en_{0e}\left(\frac{1}{c}\frac{\partial A_\parallel}{\partial t} + \boldsymbol{\nabla}_\parallel \phi\right).$$

Model equations

- Anisotropy of fluctuations $k_\parallel \ll k_\perp$ appears to be well-satisfied at small scales in the solar wind (Chen et al., 2013; Chen, 2016) $\Rightarrow$ gyrokinetics
- Two more simplifications:
  1. $\beta_e \lesssim 1$: Kinetic Reduced Electron Heating Model (KREHM)
  2. Ignore electron kinetics: isothermal KREHM
- Closed fluid system:

$$\boxed{\begin{aligned} &\frac{\mathrm{d}}{\mathrm{d}t}\bar{\tau}^{-1}\frac{e\phi}{T_{0e}} - \frac{c}{4\pi e n_{0e}}\nabla_\parallel \nabla_\perp^2 A_\parallel = 0, \\ &\frac{\mathrm{d}}{\mathrm{d}t}\left(A_\parallel - d_e^2 \nabla_\perp^2 A_\parallel\right) = -c\left(\frac{\partial\phi}{\partial z} + \nabla_\parallel \bar{\tau}^{-1}\phi\right). \end{aligned}}$$

Model equations

- Anisotropy of fluctuations $k_\parallel \ll k_\perp$ appears to be well-satisfied at small scales in the solar wind (Chen et al., 2013; Chen, 2016) $\Rightarrow$ gyrokinetics
- Two more simplifications:
  1. $\beta_e \lesssim 1$: Kinetic Reduced Electron Heating Model (KREHM)
  2. Ignore electron kinetics: isothermal KREHM
- Closed fluid system:

$$\frac{\mathrm{d}}{\mathrm{d}t}\bar{\tau}^{-1}\frac{e\phi}{T_{0e}} - \frac{c}{4\pi e n_{0e}}\nabla_\parallel \nabla_\perp^2 A_\parallel = 0,$$
$$\frac{\mathrm{d}}{\mathrm{d}t}\left(A_\parallel - d_e^2 \nabla_\perp^2 A_\parallel\right) = -c\left(\frac{\partial\phi}{\partial z} + \nabla_\parallel \bar{\tau}^{-1}\phi\right).$$

- Perpendicular scales:

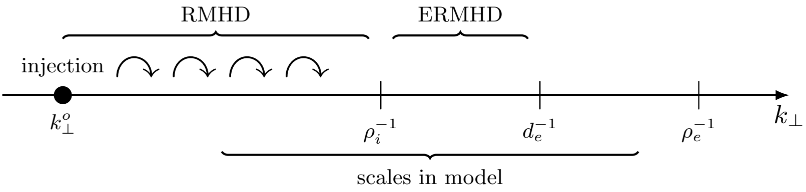

A brief aside on reduced-magnetohydrodynamics (RMHD)

- For $k_\perp \ll \rho_i^{-1}, d_e^{-1}$, we recover the equations of RMHD:

$$\frac{\partial \boldsymbol{z}^\pm}{\partial t} \pm v_A \frac{\partial \boldsymbol{z}^\pm}{\partial z} + \boldsymbol{z}^\mp \cdot \boldsymbol{\nabla}_\perp \boldsymbol{z}^\pm = 0,$$

  where

$$\boldsymbol{z}^\pm = \boldsymbol{u}_\perp \pm \frac{\delta \boldsymbol{B}_\perp}{\sqrt{4\pi n_{0i} m_i}}.$$

- Describes nonlinear dynamics of backwards/forwards propagating Alfvén waves ($\omega = \pm k_\parallel v_A$).

A brief aside on reduced-magnetohydrodynamics (RMHD)

- For $k_\perp \ll \rho_i^{-1}, d_e^{-1}$, we recover the equations of RMHD:

$$\frac{\partial \boldsymbol{z}^\pm}{\partial t} \pm v_A \frac{\partial \boldsymbol{z}^\pm}{\partial z} + \boldsymbol{z}^\mp \cdot \boldsymbol{\nabla}_\perp \boldsymbol{z}^\pm = 0,$$

  where

$$\boldsymbol{z}^\pm = \boldsymbol{u}_\perp \pm \frac{\delta \boldsymbol{B}_\perp}{\sqrt{4\pi n_{0i} m_i}}.$$

- Describes nonlinear dynamics of backwards/forwards propagating Alfvén waves ($\omega = \pm k_\parallel v_A$).
- Conserves the sum and difference of the $\boldsymbol{z}^\pm$ energies:

$$W = \frac{n_{0i} m_i}{4} \int \frac{\mathrm{d}^3 \boldsymbol{r}}{V} \left(\left|\boldsymbol{z}^+\right|^2 + \left|\boldsymbol{z}^-\right|^2 \right),$$

$$H = \frac{n_{0i} m_i}{4} \int \frac{\mathrm{d}^3 \boldsymbol{r}}{V} \left(\left|\boldsymbol{z}^+\right|^2 - \left|\boldsymbol{z}^-\right|^2 \right).$$

- Turbulence requires there to be some non-zero cross-helicity $H \Rightarrow$ non-zero *imbalance*.

Imbalance in the solar wind

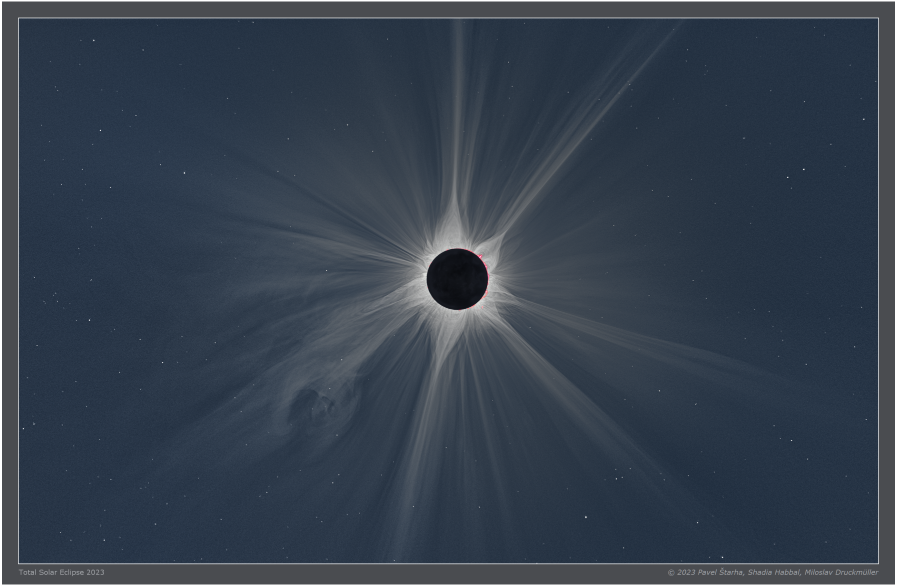

Imbalance in the solar wind

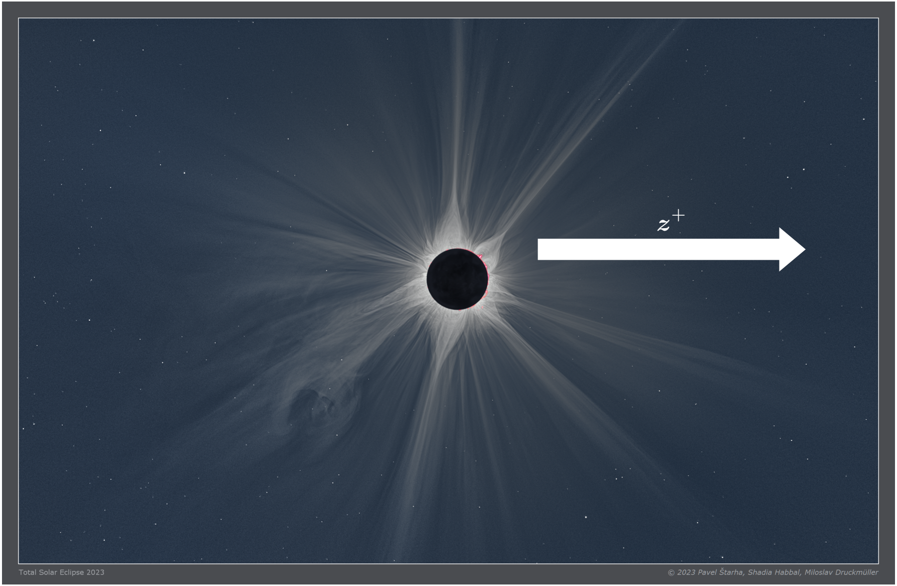

Imbalance in the solar wind

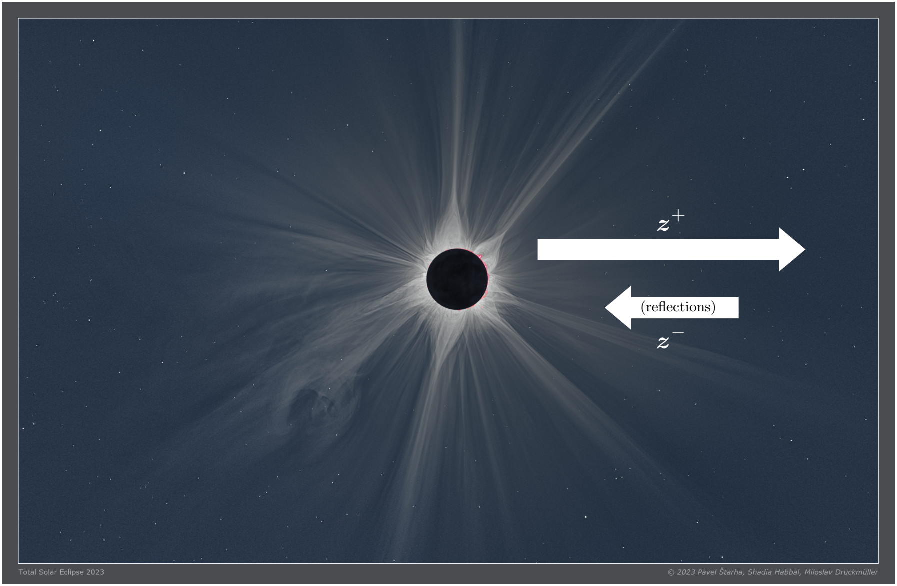

Imbalance in the solar wind

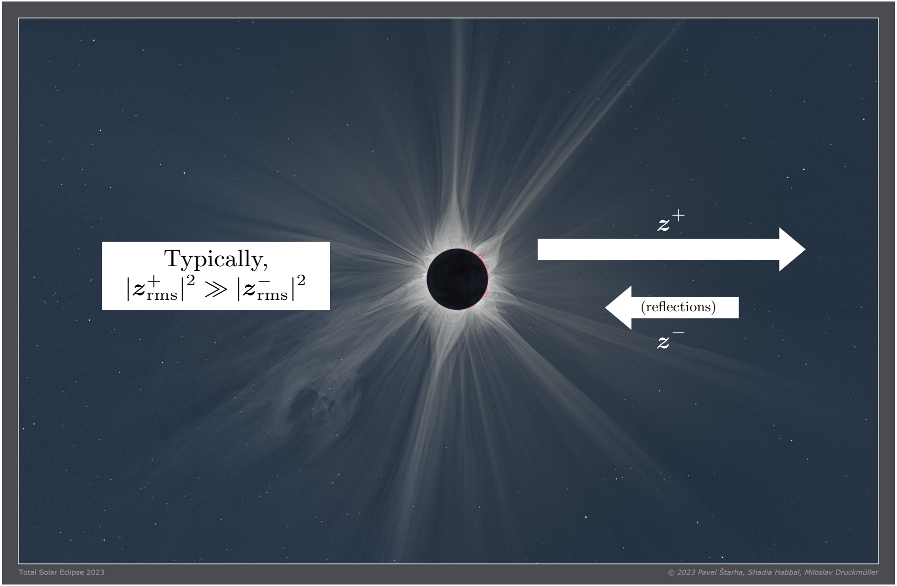

Imbalance in the solar wind

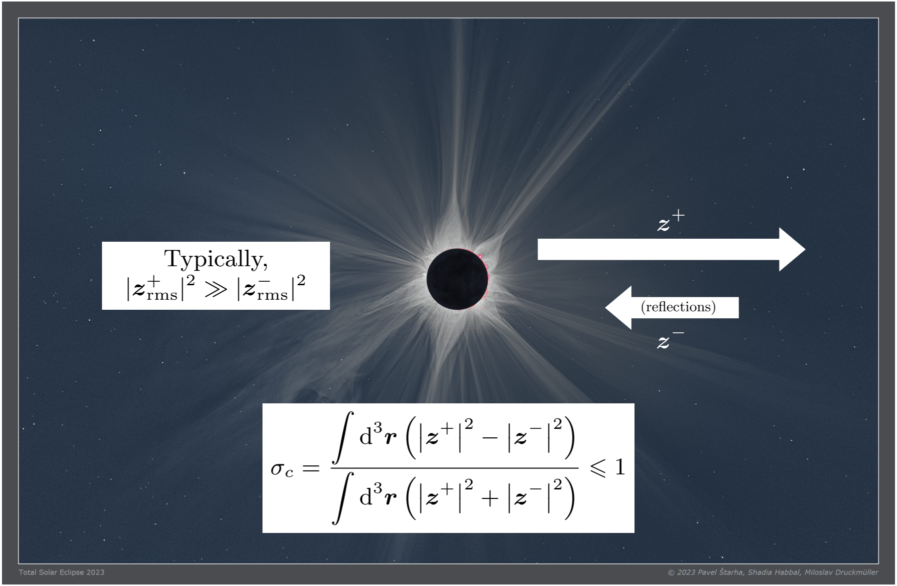

Imbalance in the solar wind

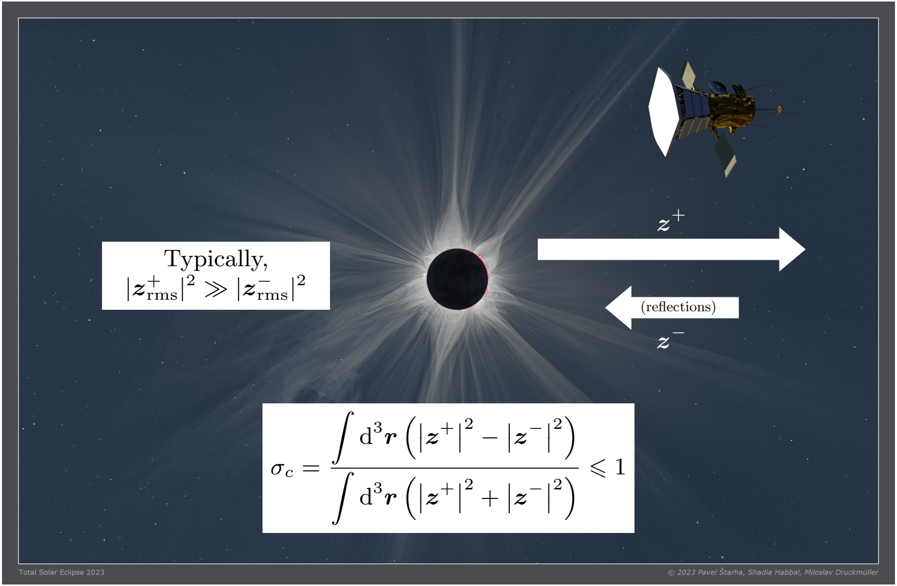

Typically,

$$|\boldsymbol{z}^+_{\rm rms}|^2 \gg |\boldsymbol{z}^-_{\rm rms}|^2$$

$$\sigma_c = \frac{\displaystyle\int \mathrm{d}^3\boldsymbol{r}\left(|\boldsymbol{z}^+|^2 - |\boldsymbol{z}^-|^2\right)}{\displaystyle\int \mathrm{d}^3\boldsymbol{r}\left(|\boldsymbol{z}^+|^2 + |\boldsymbol{z}^-|^2\right)} \leqslant 1$$

Phase velocity (isothermal KREHM)

- Forward and backwards propagating waves:

$$\omega = \pm k_\parallel v_{\rm ph}(k_\perp), \quad v_{\rm ph}(k_\perp) = k_\perp \rho_i \left(\frac{1+\bar{\tau}}{1+k_\perp^2 d_e^2} \right)^{1/2} v_A.$$

Phase velocity (isothermal KREHM)

- Forward and backwards propagating waves:

$$\omega = \pm k_\parallel v_{\rm ph}(k_\perp), \quad v_{\rm ph}(k_\perp) = k_\perp \rho_i \left(\frac{1+\bar{\tau}}{1+k_\perp^2 d_e^2} \right)^{1/2} v_A.$$

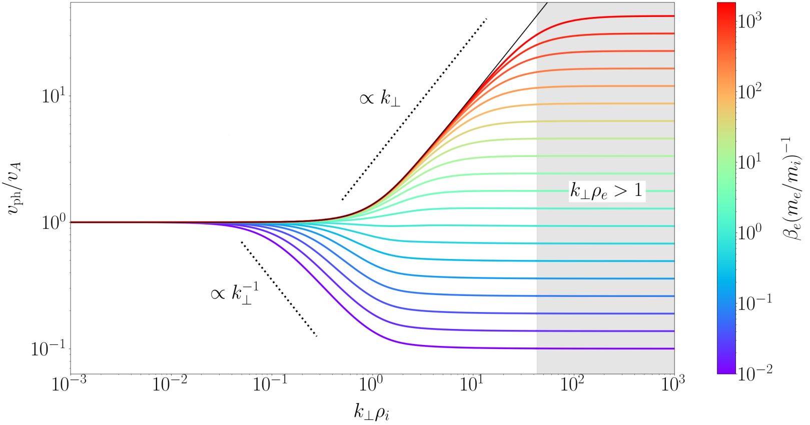

Nonlinear invariants (isothermal KREHM)

- Generalised Elsässer potentials:

$$\boldsymbol{z}^{\pm} = \lim_{k_\perp \to 0} \boldsymbol{b}_0 \times \boldsymbol{\nabla}_\perp \Theta^{\pm}.$$

- Free energy:

$$\lim_{k_\perp \to 0} W = \frac{n_{0i} m_i}{4} \int \frac{\mathrm{d}^3\boldsymbol{r}}{V} \left(\left| \boldsymbol{z}^+ \right|^2 + \left| \boldsymbol{z}^- \right|^2 \right).$$

- Generalised helicity:

$$\lim_{k_\perp \to 0} H = \frac{n_{0i} m_i}{4} \int \frac{\mathrm{d}^3\boldsymbol{r}}{V} \left(\left| \boldsymbol{z}^+ \right|^2 - \left| \boldsymbol{z}^- \right|^2 \right).$$

Nonlinear invariants (isothermal KREHM)

- Generalised Elsässer potentials:

$$\lim_{k_\perp \to 0} \Theta^{\pm}_{\boldsymbol{k}} = \frac{c}{B_0}\phi_{\boldsymbol{k}} \mp \frac{A_{\parallel \boldsymbol{k}}}{\sqrt{4\pi n_{0i} m_i}}.$$

- Free energy:

$$\lim_{k_\perp \to 0} W = \frac{n_{0i} m_i}{4} \sum_{\boldsymbol{k}} \left(\left| k_\perp \Theta^{+}_{\boldsymbol{k}} \right|^2 + \left| k_\perp \Theta^{-}_{\boldsymbol{k}} \right|^2 \right).$$

- Generalised helicity:

$$\lim_{k_\perp \to 0} H = \frac{n_{0i} m_i}{4} \sum_{\boldsymbol{k}} \left(\left| k_\perp \Theta^{+}_{\boldsymbol{k}} \right|^2 - \left| k_\perp \Theta^{-}_{\boldsymbol{k}} \right|^2 \right).$$

Nonlinear invariants (isothermal KREHM)

- Generalised Elsässer potentials:

$$\Theta_{\boldsymbol{k}}^{\pm} \equiv \sqrt{1 + k_\perp^2 d_e^2} \left[\frac{c}{B_0} \frac{v_{\rm ph}(k_\perp)/v_A}{(k_\perp \rho_s)^2} \bar{\tau}^{-1} \phi_{\boldsymbol{k}} \mp \frac{A_{\parallel \boldsymbol{k}}}{\sqrt{4\pi n_{0i} m_i}} \right].$$

- Free energy:

$$W = \frac{n_{0i} m_i}{4} \sum_{\boldsymbol{k}} \left(\left| k_\perp \Theta_{\boldsymbol{k}}^{+} \right|^2 + \left| k_\perp \Theta_{\boldsymbol{k}}^{-} \right|^2 \right).$$

- Generalised helicity:

$$H = \frac{n_{0i} m_i}{4} \sum_{\boldsymbol{k}} \frac{\left| k_\perp \Theta_{\boldsymbol{k}}^{+} \right|^2 - \left| k_\perp \Theta_{\boldsymbol{k}}^{-} \right|^2}{v_{\rm ph}(k_\perp)/v_A}.$$

Nonlinear invariants (isothermal KREHM)

- Generalised Elsässer potentials:

$$\Theta_{\boldsymbol{k}}^{\pm} \equiv \sqrt{1 + k_\perp^2 d_e^2} \left[\frac{c}{B_0} \frac{v_{\rm ph}(k_\perp)/v_A}{(k_\perp \rho_s)^2} \bar{\tau}^{-1} \phi_{\boldsymbol{k}} \mp \frac{A_{\parallel \boldsymbol{k}}}{\sqrt{4\pi n_{0i} m_i}} \right].$$

- Free energy:

$$W = \frac{n_{0i} m_i}{4} \sum_{\boldsymbol{k}} \left(\left| k_\perp \Theta_{\boldsymbol{k}}^{+} \right|^2 + \left| k_\perp \Theta_{\boldsymbol{k}}^{-} \right|^2 \right).$$

- Generalised helicity:

$$H = \frac{n_{0i} m_i}{4} \sum_{\boldsymbol{k}} \frac{\left| k_\perp \Theta_{\boldsymbol{k}}^{+} \right|^2 - \left| k_\perp \Theta_{\boldsymbol{k}}^{-} \right|^2}{v_{\rm ph}(k_\perp)/v_A}.$$

- Existence of two nonlinear invariants constrains the dynamical states accessible to the system. **What are these states, and how do they arise? What are the consequences for turbulent heating?**

Constant-flux cascade

- Free energy and generalised helicity are injected at the constant rates ε_W and ε_H, respectively, with **injection imbalance** $\sigma_\varepsilon = |\varepsilon_H|/\varepsilon_W$.

Constant-flux cascade

- Free energy and generalised helicity are injected at the constant rates ε_W and ε_H, respectively, with **injection imbalance** $\sigma_\varepsilon = |\varepsilon_H|/\varepsilon_W$.
- Assuming a constant flux of energy to small scales, one can derive scalings for the perpendicular energy spectra $E^\pm(k_\perp)$, $E^K(k_\perp)$, and $E^B(k_\perp)$.

Constant-flux cascade

- Free energy and generalised helicity are injected at the constant rates ε_W and ε_H, respectively, with **injection imbalance** $\sigma_\varepsilon = |\varepsilon_H|/\varepsilon_W$.
- Assuming a constant flux of energy to small scales, one can derive scalings for the perpendicular energy spectra $E^\pm(k_\perp)$, $E^K(k_\perp)$, and $E^B(k_\perp)$.

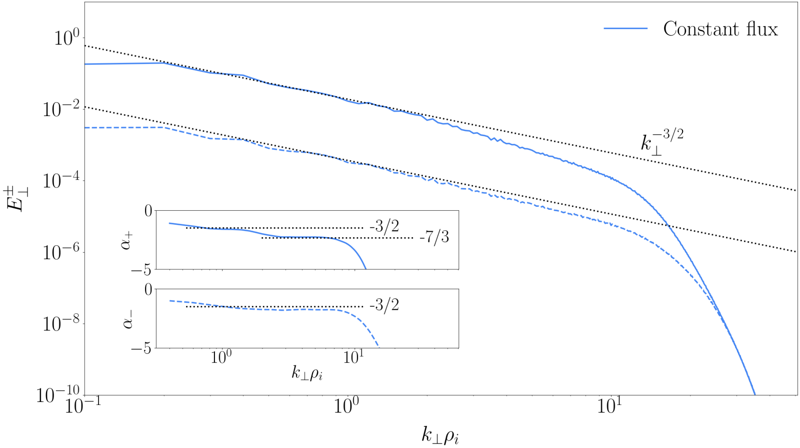

Constant-flux cascade

- Free energy and generalised helicity are injected at the constant rates ε_W and ε_H, respectively, with **injection imbalance** $\sigma_\varepsilon = |\varepsilon_H|/\varepsilon_W$.
- Assuming a constant flux of energy to small scales, one can derive scalings for the perpendicular energy spectra $E^{\pm}(k_\perp)$, $E^K(k_\perp)$, and $E^B(k_\perp)$.

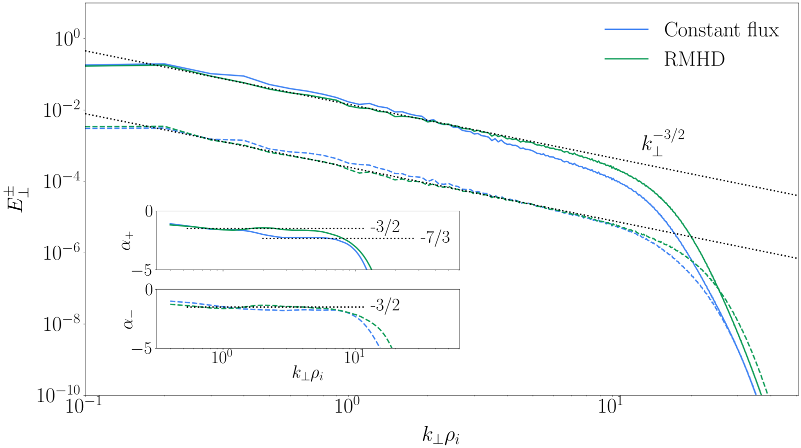

Constant-flux cascade

- Free energy and generalised helicity are injected at the constant rates ε_W and ε_H, respectively, with **injection imbalance** $\sigma_\varepsilon = |\varepsilon_H|/\varepsilon_W$.
- Assuming a constant flux of energy to small scales, one can derive scalings for the perpendicular energy spectra $E^\pm(k_\perp)$, $E^K(k_\perp)$, and $E^B(k_\perp)$.

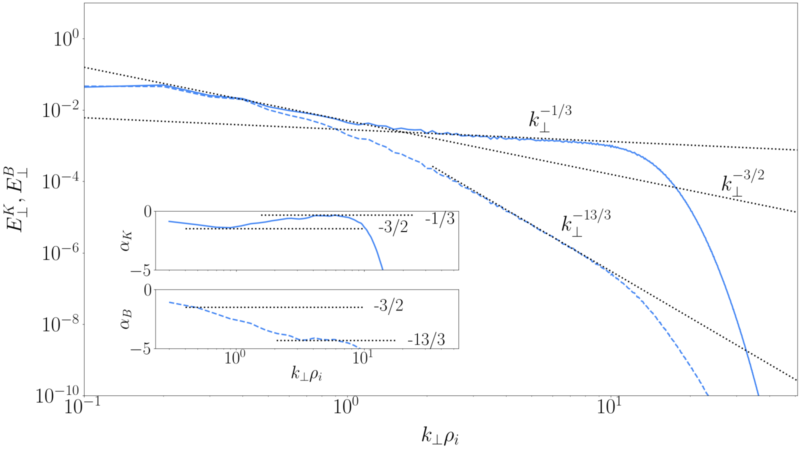

Effect of helicity conservation

- Free energy and generalised helicity are injected at the **constant** rates ε_W and ε_H, respectively.
- Then, estimate

$$\frac{\mathrm{d}W}{\mathrm{d}t} \propto t_{\mathrm{nl}}^{-1} \left(\phi_{k_\perp}\right)^2 \sim \varepsilon_W ,$$

and

$$\frac{\mathrm{d}H}{\mathrm{d}t} \propto t_{\mathrm{nl}}^{-1} \left(\phi_{k_\perp}\right) \left(A_{\parallel k_\perp}\right) \cos\alpha_{k_\perp} \sim \varepsilon_H ,$$

where

$$\cos\alpha_{k_\perp} = \frac{\overline{\mathrm{Re}\left\langle \phi_{\boldsymbol{k}} (A_{\parallel \boldsymbol{k}})^* \right\rangle}}{\left(\overline{\langle |\phi_{\boldsymbol{k}}|^2 \rangle}\right)^{1/2} \left(\overline{\langle |A_{\parallel \boldsymbol{k}}|^2 \rangle}\right)^{1/2}} .$$

- Using equipartition to relate the amplitudes of ϕ and $A_\parallel$, we find...

Effect of helicity conservation

- ... a condition for the existence of a constant-flux cascade! ($\varepsilon_H \leqslant \varepsilon_W$)

$$\varepsilon_H \sim \varepsilon_W \left(\frac{v_{\rm ph}}{v_A}\right)^{-1} \cos\alpha_{k_\perp} \quad \Rightarrow \quad \boxed{\sigma_\varepsilon \frac{v_{\rm ph}(k_\perp)}{v_A} \lesssim 1.}$$

Effect of helicity conservation

- ... a condition for the existence of a constant-flux cascade! ($\varepsilon_H \leqslant \varepsilon_W$)

$$\varepsilon_H \sim \varepsilon_W \left(\frac{v_{\rm ph}}{v_A}\right)^{-1} \cos\alpha_{k_\perp} \quad \Rightarrow \quad \boxed{\sigma_\varepsilon \frac{v_{\rm ph}(k_\perp)}{v_A} \lesssim 1.}$$

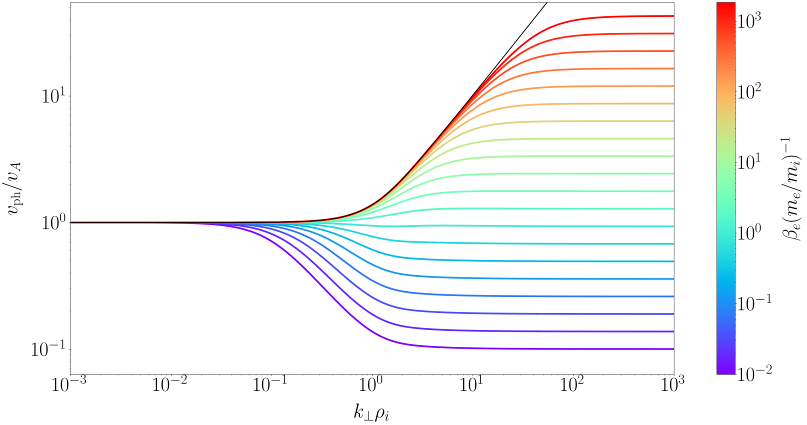

Effect of helicity conservation

- ... a condition for the existence of a constant-flux cascade! ($\varepsilon_H \leqslant \varepsilon_W$)

$$\varepsilon_H \sim \varepsilon_W \left(\frac{v_{\rm ph}}{v_A}\right)^{-1} \cos\alpha_{k_\perp} \quad \Rightarrow \quad \boxed{\sigma_\varepsilon \frac{v_{\rm ph}(k_\perp)}{v_A} \lesssim 1.}$$

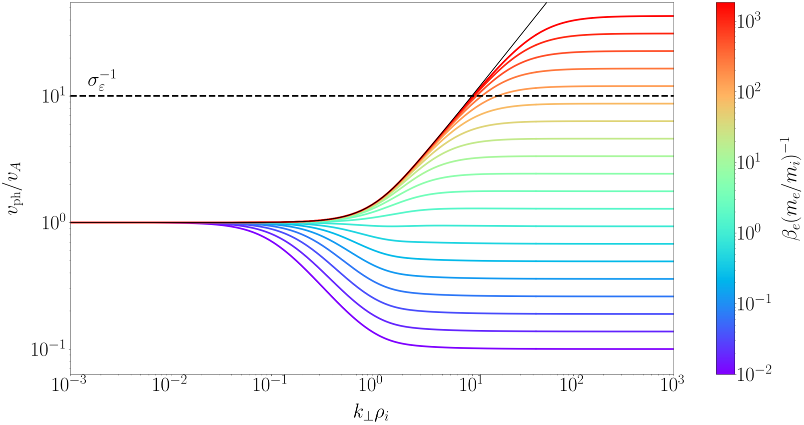

Effect of helicity conservation

- ... a condition for the existence of a constant-flux cascade! $(\varepsilon_H \leqslant \varepsilon_W)$

$$\varepsilon_H \sim \varepsilon_W \left(\frac{v_{\rm ph}}{v_A}\right)^{-1} \cos\alpha_{k_\perp} \quad \Rightarrow \quad \boxed{\sigma_\varepsilon \frac{v_{\rm ph}(k_\perp)}{v_A} \lesssim 1.}$$

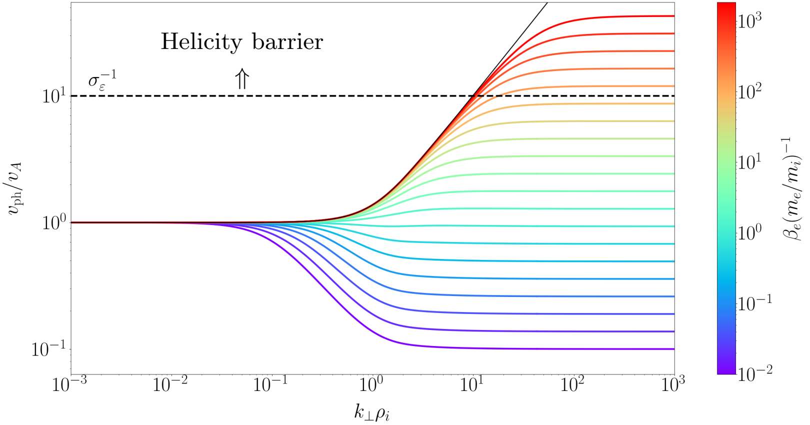

Effect of helicity conservation

- ... a condition for the existence of a constant-flux cascade! $(\varepsilon_H \leqslant \varepsilon_W)$

$$\varepsilon_H \sim \varepsilon_W \left(\frac{v_{\rm ph}}{v_A}\right)^{-1} \cos\alpha_{k_\perp} \quad \Rightarrow \quad \boxed{\sigma_\varepsilon \frac{v_{\rm ph}(k_\perp)}{v_A} \lesssim 1.}$$

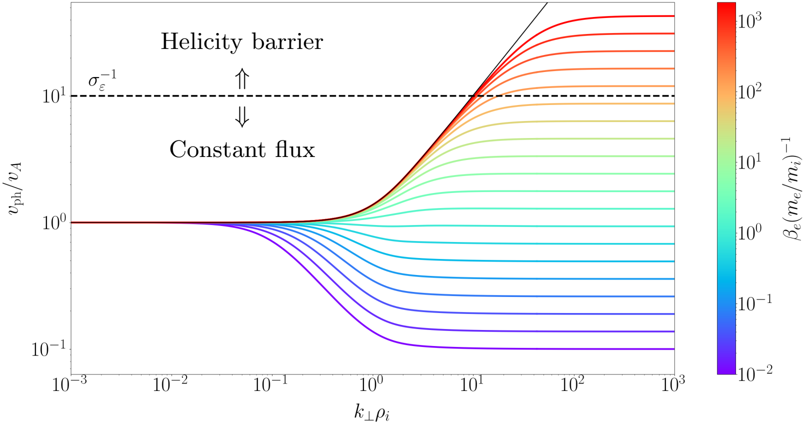

Effect of helicity conservation

- ... a condition for the existence of a constant-flux cascade! ($\varepsilon_H \leqslant \varepsilon_W$)

$$\varepsilon_H \sim \varepsilon_W \left(\frac{v_{\rm ph}}{v_A}\right)^{-1} \cos\alpha_{k_\perp} \quad \Rightarrow \quad \boxed{\sigma_\varepsilon \frac{v_{\rm ph}(k_\perp)}{v_A} \lesssim 1.}$$

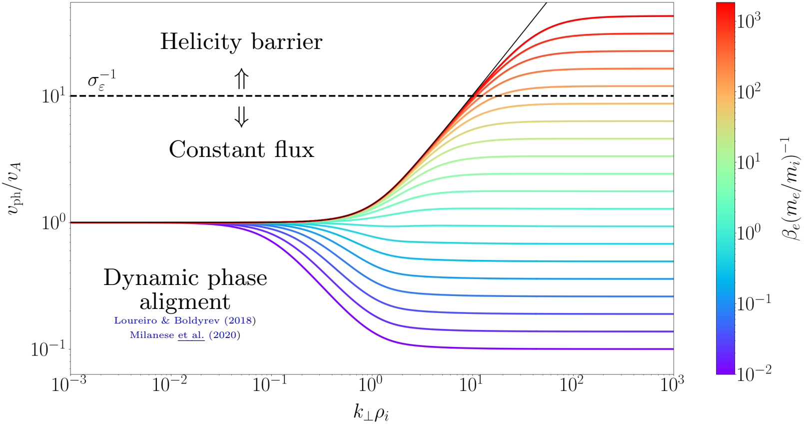

Effect of helicity conservation

- ... a condition for the existence of a constant-flux cascade! $(\varepsilon_H \leqslant \varepsilon_W)$

$$\varepsilon_H \sim \varepsilon_W \left(\frac{v_{\rm ph}}{v_A}\right)^{-1} \cos\alpha_{k_\perp} \quad \Rightarrow \quad \boxed{\sigma_\varepsilon \frac{v_{\rm ph}(k_\perp)}{v_A} \lesssim 1.}$$

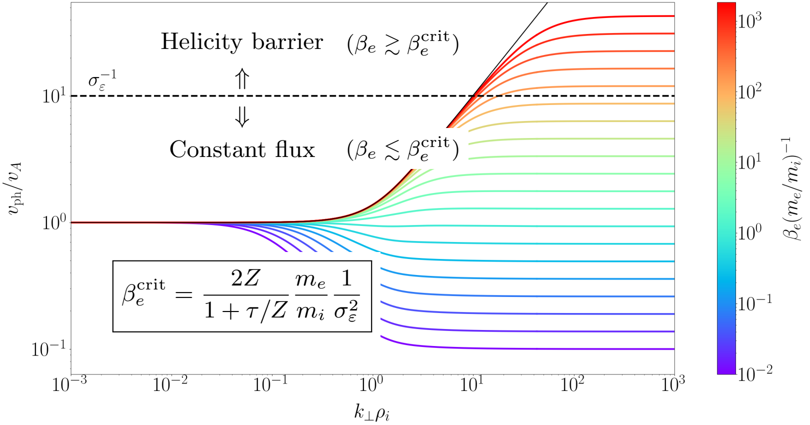

Effect of helicity conservation

- … a condition for the existence of a constant-flux cascade! $(\varepsilon_H \leqslant \varepsilon_W)$

$$\varepsilon_H \sim \varepsilon_W \left(\frac{v_{\rm ph}}{v_A}\right)^{-1} \cos\alpha_{k_\perp} \quad \Rightarrow \quad \boxed{\sigma_\varepsilon \frac{v_{\rm ph}(k_\perp)}{v_A} \lesssim 1.}$$

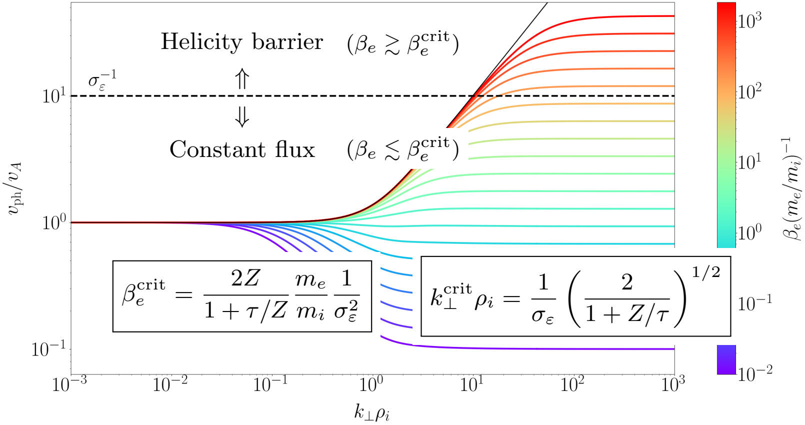

$$\boxed{\beta_e^{\rm crit} = \frac{2Z}{1+\tau/Z}\frac{m_e}{m_i}\frac{1}{\sigma_\varepsilon^2}}$$

$$\boxed{k_\perp^{\rm crit}\rho_i = \frac{1}{\sigma_\varepsilon}\left(\frac{2}{1+Z/\tau}\right)^{1/2}}$$

Features of the helicity barrier

- Compare two otherwise identical simulations with $\sigma_\varepsilon = 0.8$:
  - Constant flux: $d_e = \rho_i$, $\beta_e/\beta_e^{\mathrm{crit}} = 0.64$
  - Helicity barrier: $d_e = \rho_i/2$, $\beta_e/\beta_e^{\mathrm{crit}} = 2.56$

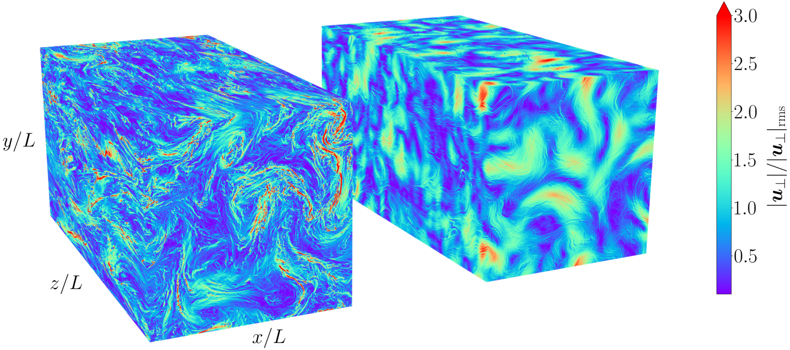

Features of the helicity barrier

1.

2.

3.

Features of the helicity barrier

1. **Nonlinear fluxes**: the helicity barrier only allows $\approx 2\varepsilon^-$ of the free energy to cascade to small scales $[\varepsilon^{\pm} = (1 \pm \sigma_\varepsilon)\varepsilon_W/2]$.
2.
3.

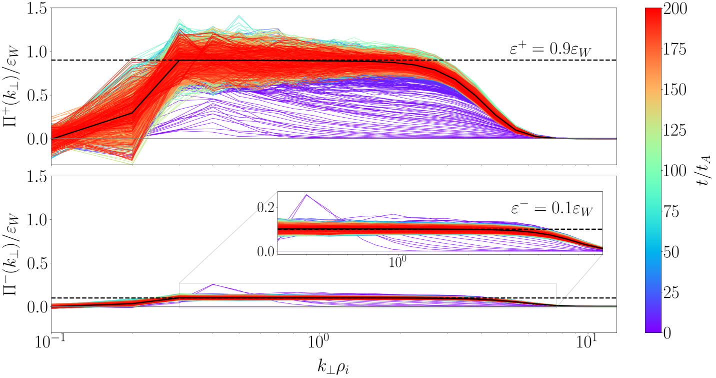

Features of the helicity barrier

1. **Nonlinear fluxes**: the helicity barrier only allows $\approx 2\varepsilon^-$ of the free energy to cascade to small scales $[\varepsilon^\pm = (1 \pm \sigma_\varepsilon)\varepsilon_W/2]$.
2.
3.

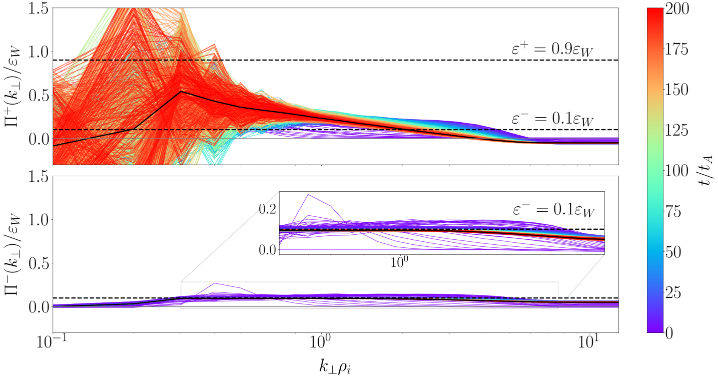

Features of the helicity barrier

1. **Nonlinear fluxes**: the helicity barrier only allows $\approx 2\varepsilon^-$ of the free energy to cascade to small scales $[\varepsilon^\pm = (1 \pm \sigma_\varepsilon)\varepsilon_W/2]$.
2.
3.

This behaviour is shared by more realistic hybrid-kinetic simulations conducted with PEGASUS++ (Squire et al., 2022)

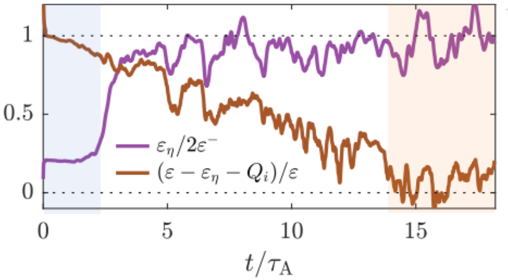

Features of the helicity barrier

1. **Nonlinear fluxes**: the helicity barrier only allows $\approx 2\varepsilon^-$ of the free energy to cascade to small scales $[\varepsilon^\pm = (1 \pm \sigma_\varepsilon)\varepsilon_W/2]$.
2. **Parallel dissipation**: energy trapped at large perpendicular scales (small $k_\perp$) dissipates on small parallel ones (large $k_\parallel$).
3.

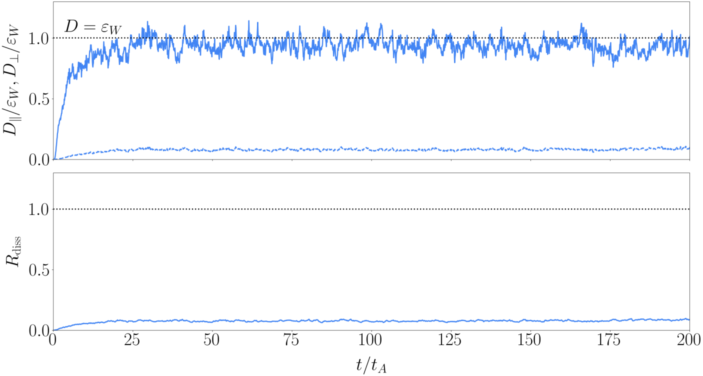

Features of the helicity barrier

1. **Nonlinear fluxes**: the helicity barrier only allows $\approx 2\varepsilon^-$ of the free energy to cascade to small scales $[\varepsilon^\pm = (1 \pm \sigma_\varepsilon)\varepsilon_W/2]$.
2. **Parallel dissipation**: energy trapped at large perpendicular scales (small $k_\perp$) dissipates on small parallel ones (large $k_\|$).
3.

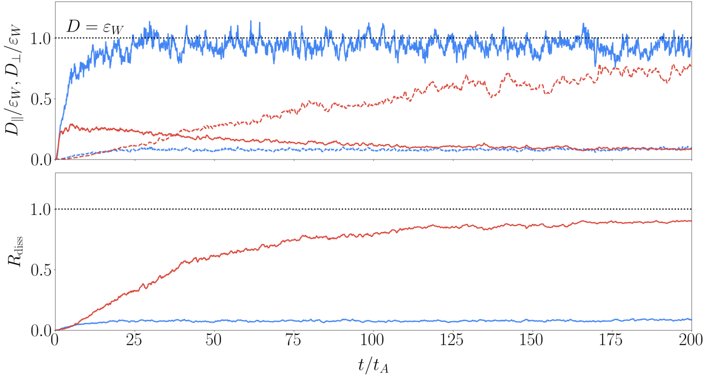

Features of the helicity barrier

1. **Nonlinear fluxes**: the helicity barrier only allows $\approx 2\varepsilon^-$ of the free energy to cascade to small scales $[\varepsilon^{\pm} = (1 \pm \sigma_\varepsilon)\varepsilon_W/2]$.
2. **Parallel dissipation**: energy trapped at large perpendicular scales (small $k_\perp$) dissipates on small parallel ones (large $k_\parallel$).
3.

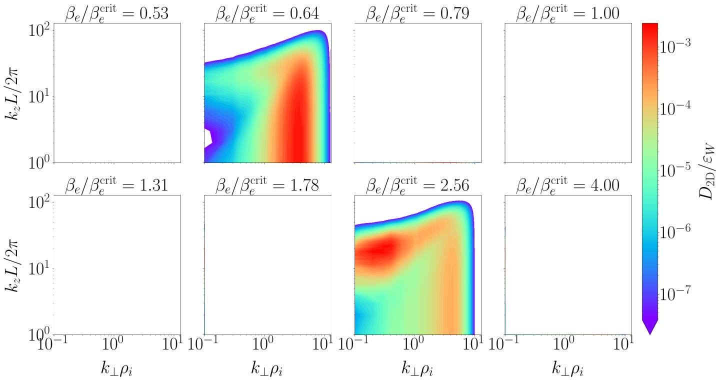

Features of the helicity barrier

1. **Nonlinear fluxes**: the helicity barrier only allows $\approx 2\varepsilon^-$ of the free energy to cascade to small scales $[\varepsilon^{\pm} = (1 \pm \sigma_\varepsilon)\varepsilon_W/2]$.
2. **Parallel dissipation**: energy trapped at large perpendicular scales (small $k_\perp$) dissipates on small parallel ones (large $k_\parallel$).
3.

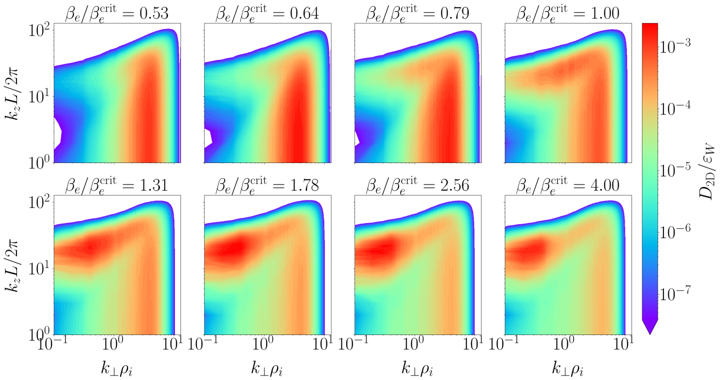

Features of the helicity barrier

1. **Nonlinear fluxes**: the helicity barrier only allows $\approx 2\varepsilon^-$ of the free energy to cascade to small scales $[\varepsilon^\pm = (1 \pm \sigma_\varepsilon)\varepsilon_W/2]$.
2. **Parallel dissipation**: energy trapped at large perpendicular scales (small $k_\perp$) dissipates on small parallel ones (large $k_\parallel$).
3.

Outside of the GK approximation, these small scales will cause parallel ion heating by exciting (resonant) ICWs (Squire et al., 2022)

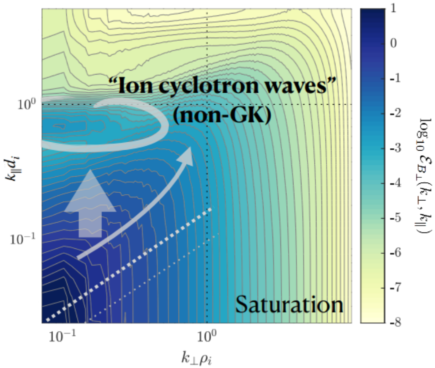

Features of the helicity barrier

1. **Nonlinear fluxes**: the helicity barrier only allows $\approx 2\varepsilon^-$ of the free energy to cascade to small scales $[\varepsilon^\pm = (1 \pm \sigma_\varepsilon)\varepsilon_W/2]$.
2. **Parallel dissipation**: energy trapped at large perpendicular scales (small $k_\perp$) dissipates on small parallel ones (large $k_\parallel$).
3. **Perpendicular energy spectra**: display a sharp spectral break with a $\sim k_\perp^{-4}$ scaling below it.

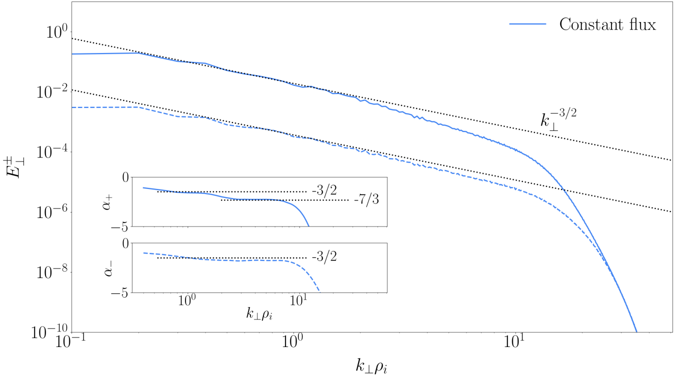

Features of the helicity barrier

1. **Nonlinear fluxes**: the helicity barrier only allows $\approx 2\varepsilon^-$ of the free energy to cascade to small scales $[\varepsilon^\pm = (1 \pm \sigma_\varepsilon)\varepsilon_W/2]$.
2. **Parallel dissipation**: energy trapped at large perpendicular scales (small $k_\perp$) dissipates on small parallel ones (large $k_\|$).
3. **Perpendicular energy spectra**: display a sharp spectral break with a $\sim k_\perp^{-4}$ scaling below it.

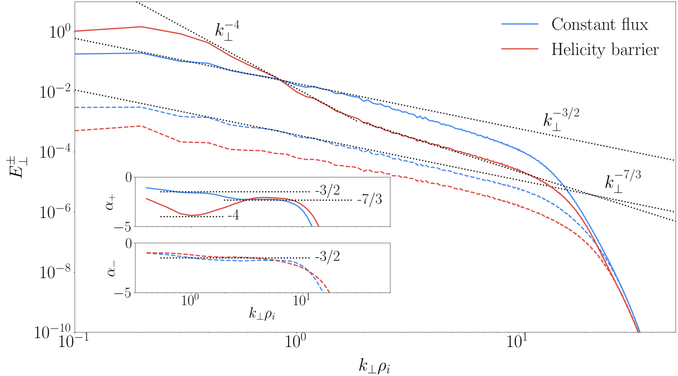

Verifying $\beta_e^{\rm crit}$ prediction

$$\boxed{\beta_e^{\rm crit} = \frac{2Z}{1+\tau/Z}\frac{m_e}{m_i}\frac{1}{\sigma_\varepsilon^2}}$$

- Test using the fact that $R_{\rm diss} = D_\parallel/(D_\perp + D_\parallel)$ is an increasing function of time in the presence of a helicity barrier.

Verifying β_e^{crit} prediction

$$\beta_e^{\mathrm{crit}} = \frac{2Z}{1+\tau/Z}\frac{m_e}{m_i}\frac{1}{\sigma_\varepsilon^2}$$

- Test using the fact that $R_{\mathrm{diss}} = D_\parallel/(D_\perp + D_\parallel)$ is an increasing function of time in the presence of a helicity barrier.

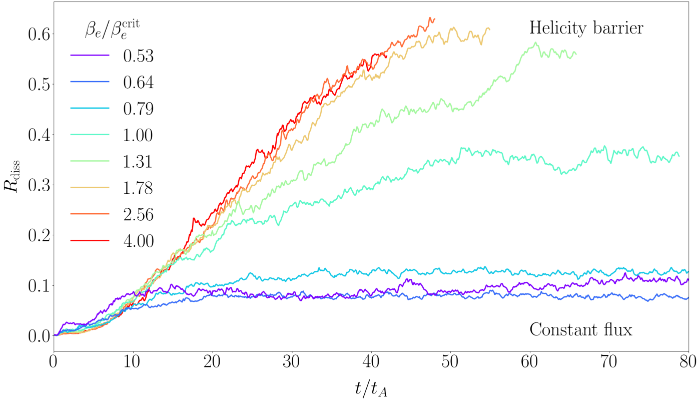

Verifying $\beta_e^{\rm crit}$ prediction

$$\beta_e^{\rm crit} = \frac{2Z}{1+\tau/Z}\frac{m_e}{m_i}\frac{1}{\sigma_\varepsilon^2}$$

- Test using the fact that $R_{\rm diss} = D_\parallel/(D_\perp + D_\parallel)$ is an increasing function of time in the presence of a helicity barrier.

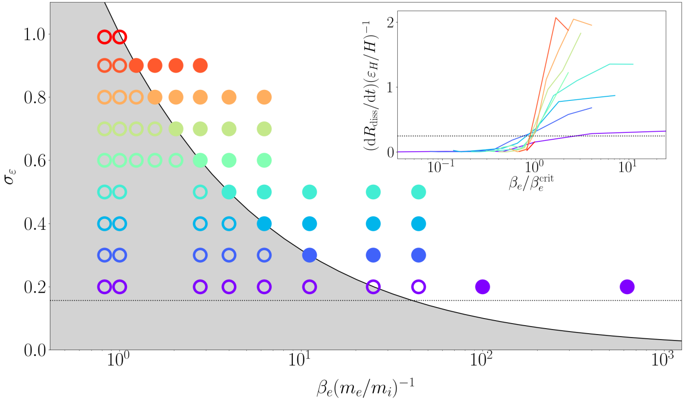

Verifying $\beta_e^{\rm crit}$ prediction

$$\boxed{k_\perp^{\rm crit}\rho_i = \frac{1}{\sigma_\varepsilon}\left(\frac{2}{1+Z/\tau}\right)^{1/2}}$$

- Test using the fact that $R_{\rm diss} = D_\parallel/(D_\perp + D_\parallel)$ is an increasing function of time in the presence of a helicity barrier.

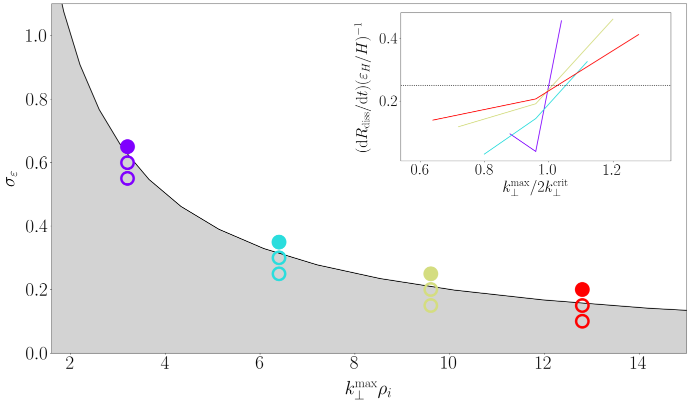

Turbulent cascade revisited (constant flux)

$$\beta_e \lesssim \beta_e^{\mathrm{crit}} = \frac{2Z}{1+\tau/Z}\frac{m_e}{m_i}\frac{1}{\sigma_\varepsilon^2}$$

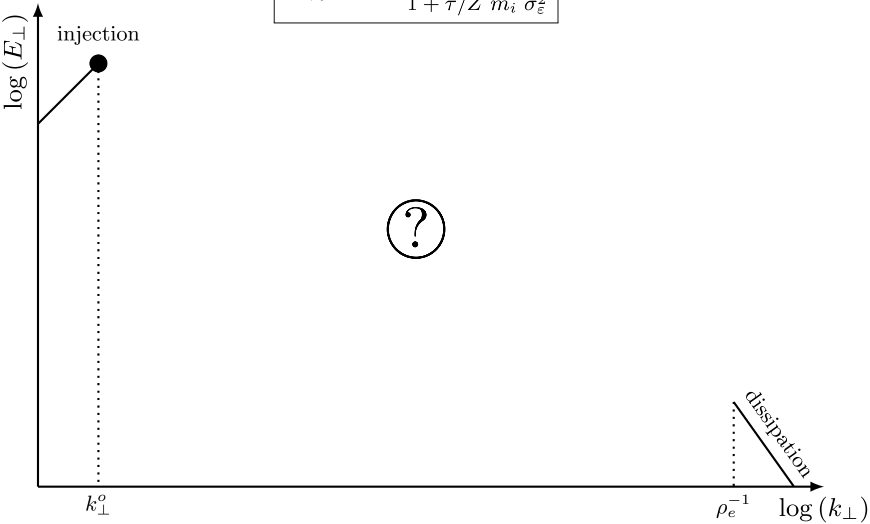

Turbulent cascade revisited (constant flux)

$$\beta_e \lesssim \beta_e^{\rm crit} = \frac{2Z}{1+\tau/Z}\frac{m_e}{m_i}\frac{1}{\sigma_\varepsilon^2}$$

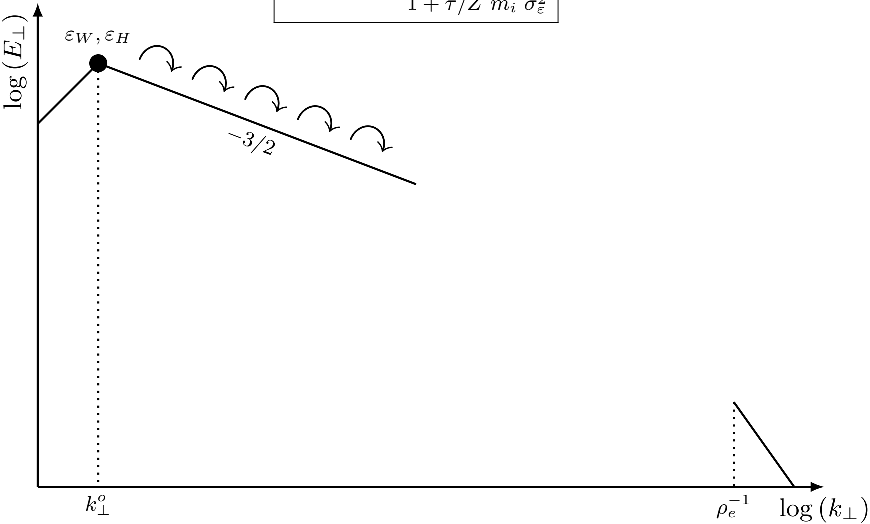

Turbulent cascade revisited (constant flux)

$$\beta_e \lesssim \beta_e^{\rm crit} = \frac{2Z}{1+\tau/Z}\frac{m_e}{m_i}\frac{1}{\sigma_\varepsilon^2}$$

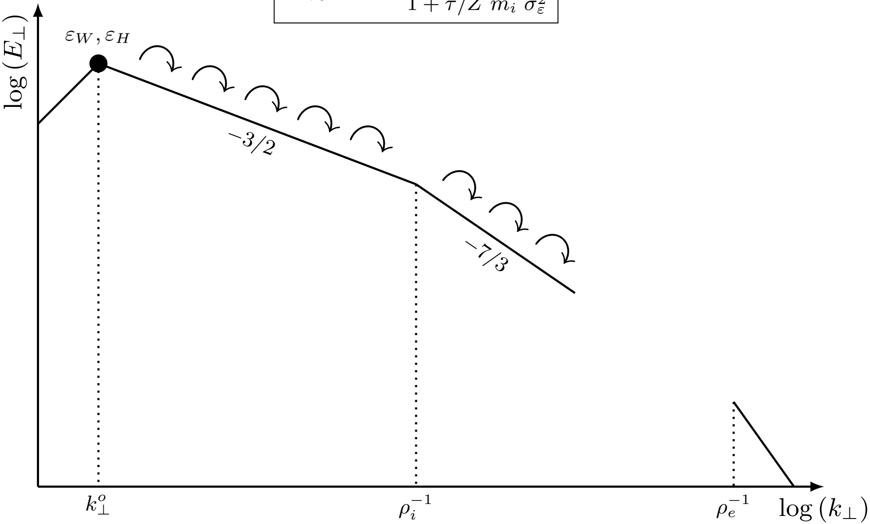

Turbulent cascade revisited (constant flux)

$$\beta_e \lesssim \beta_e^{\rm crit} = \frac{2Z}{1+\tau/Z}\frac{m_e}{m_i}\frac{1}{\sigma_\varepsilon^2}$$

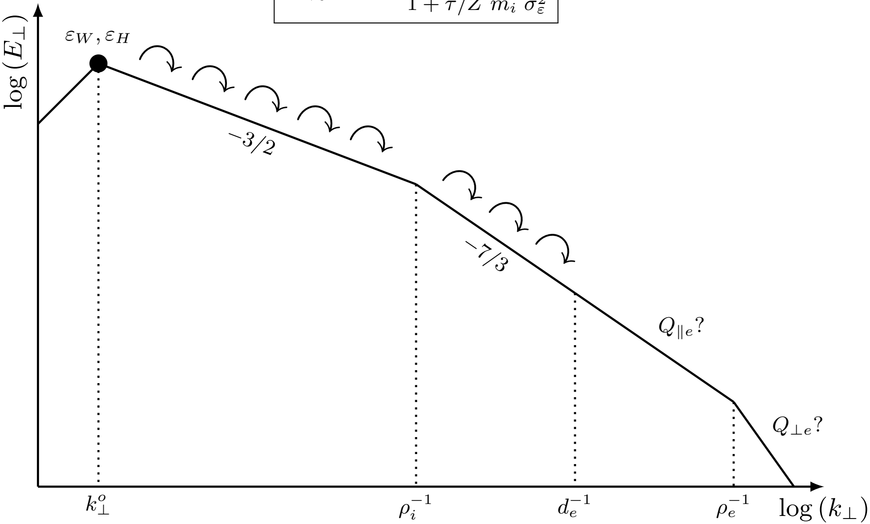

Turbulent cascade revisited (constant flux)

$$\beta_e \lesssim \beta_e^{\text{crit}} = \frac{2Z}{1+\tau/Z}\frac{m_e}{m_i}\frac{1}{\sigma_\varepsilon^2}$$

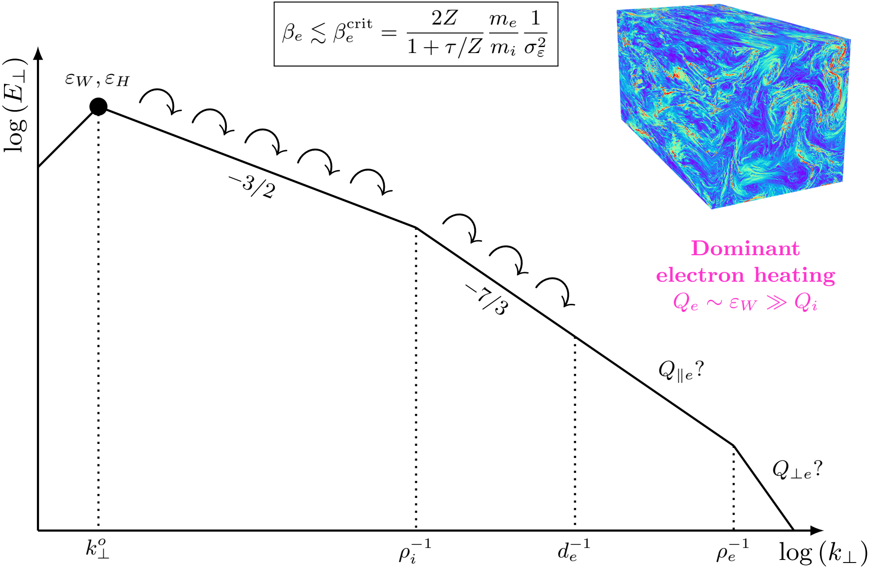

Dominant electron heating
$Q_e \sim \varepsilon_W \gg Q_i$

Turbulent cascade revisited (helicity barrier)

$$\beta_e \gtrsim \beta_e^{\rm crit} = \frac{2Z}{1+\tau/Z}\frac{m_e}{m_i}\frac{1}{\sigma_\varepsilon^2}$$

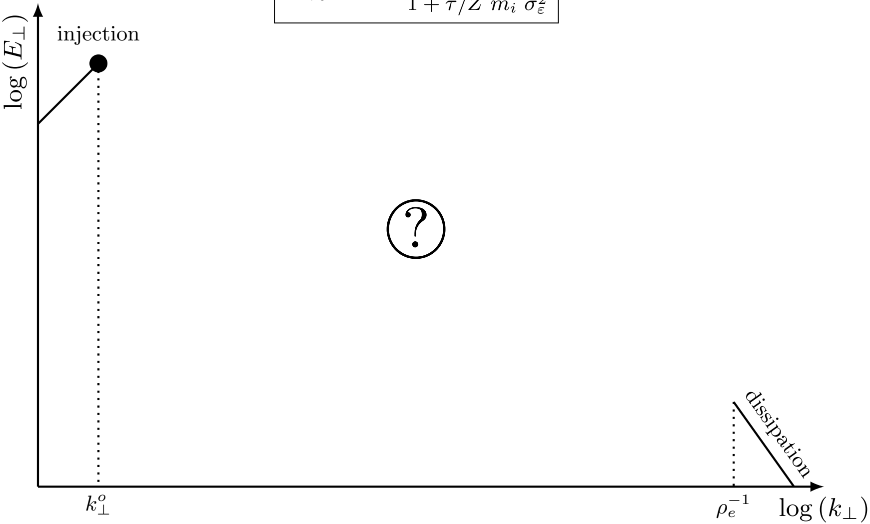

Turbulent cascade revisited (helicity barrier)

$$\beta_e \gtrsim \beta_e^{\rm crit} = \frac{2Z}{1+\tau/Z}\frac{m_e}{m_i}\frac{1}{\sigma_\varepsilon^2}$$

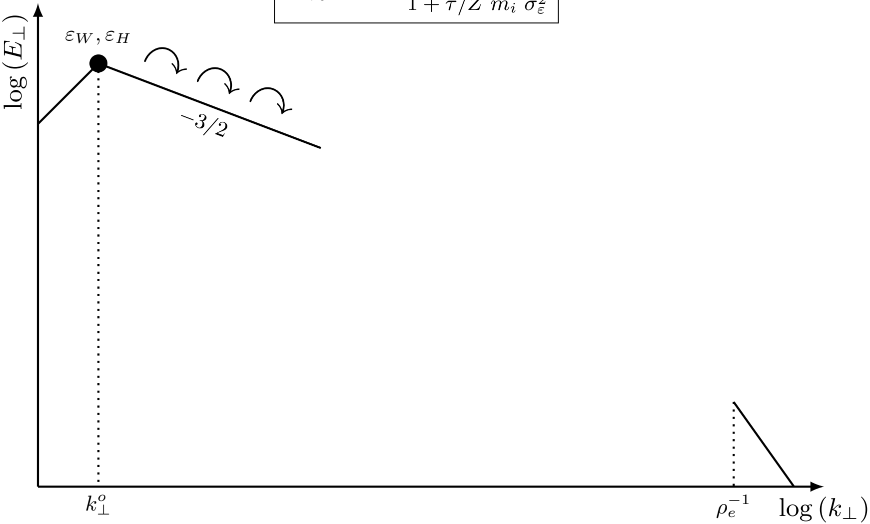

Turbulent cascade revisited (helicity barrier)

$$\beta_e \gtrsim \beta_e^{\mathrm{crit}} = \frac{2Z}{1+\tau/Z}\frac{m_e}{m_i}\frac{1}{\sigma_\varepsilon^2}$$

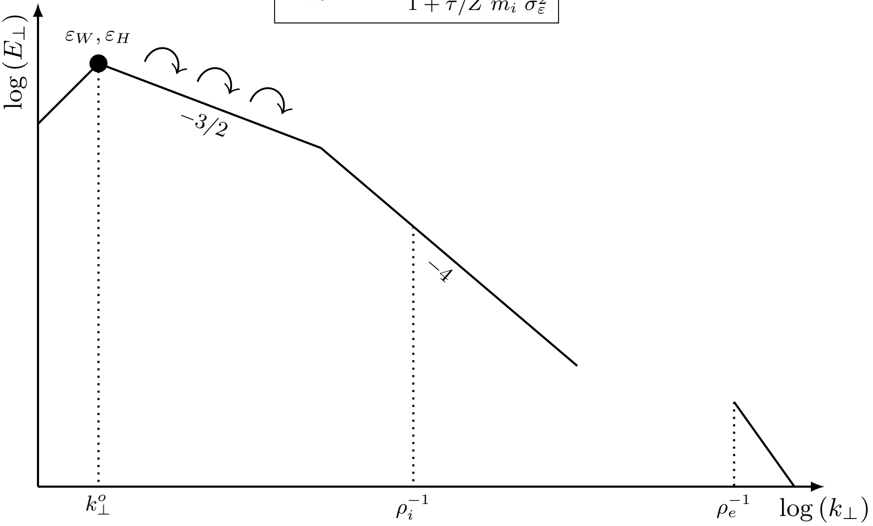

Turbulent cascade revisited (helicity barrier)

$$\beta_e \gtrsim \beta_e^{\rm crit} = \frac{2Z}{1+\tau/Z}\frac{m_e}{m_i}\frac{1}{\sigma_\varepsilon^2}$$

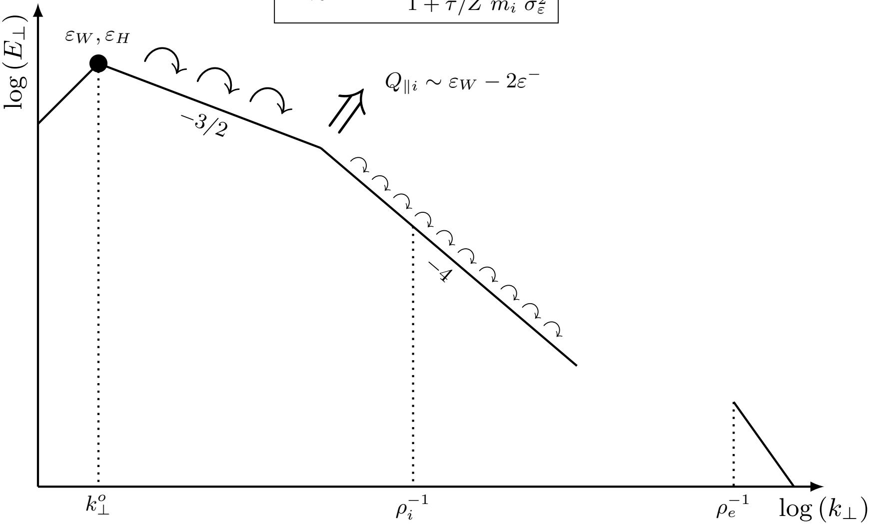

Turbulent cascade revisited (helicity barrier)

$$\beta_e \gtrsim \beta_e^{\text{crit}} = \frac{2Z}{1+\tau/Z}\frac{m_e}{m_i}\frac{1}{\sigma_\varepsilon^2}$$

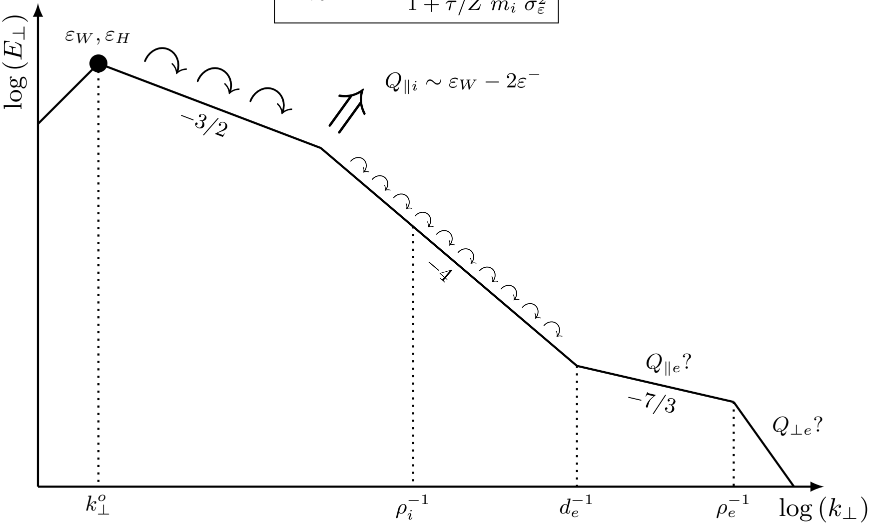

Turbulent cascade revisited (helicity barrier)

$$\beta_e \gtrsim \beta_e^{\mathrm{crit}} = \frac{2Z}{1+\tau/Z}\frac{m_e}{m_i}\frac{1}{\sigma_\varepsilon^2}$$

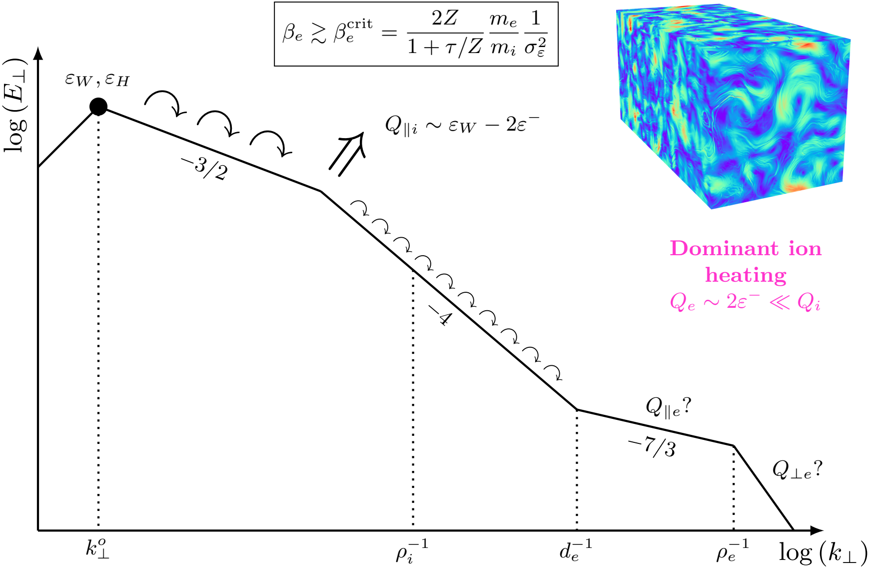

Dominant ion heating

$Q_e \sim 2\varepsilon^- \ll Q_i$

Helicity barrier "in situ"

- The (fast) solar wind generally has $\beta_e \gg \beta_e^{\mathrm{crit}}$, and so we would expect to see observational signatures of the helicity barrier.

Helicity barrier "in situ"

- The (fast) solar wind generally has $\beta_e \gg \beta_e^{\text{crit}}$, and so we would expect to see observational signatures of the helicity barrier.

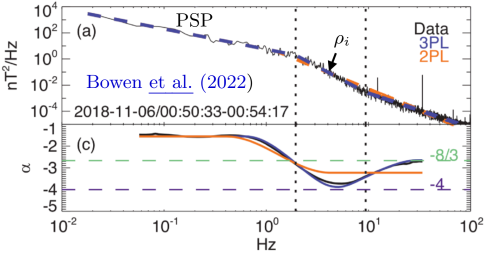

Helicity barrier "in situ"

- The (fast) solar wind generally has $\beta_e \gg \beta_e^{\mathrm{crit}}$, and so we would expect to see observational signatures of the helicity barrier.

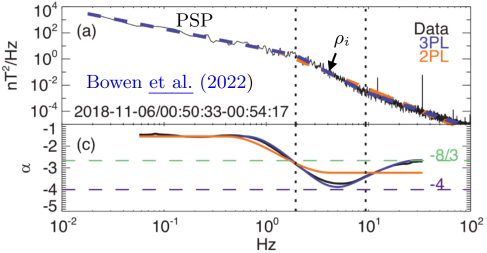

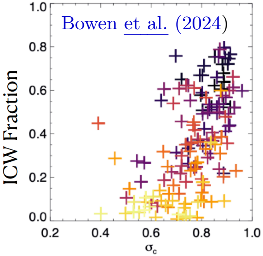

Helicity barrier "in situ"

- The (fast) solar wind generally has $\beta_e \gg \beta_e^{\mathrm{crit}}$, and so we would expect to see observational signatures of the helicity barrier.

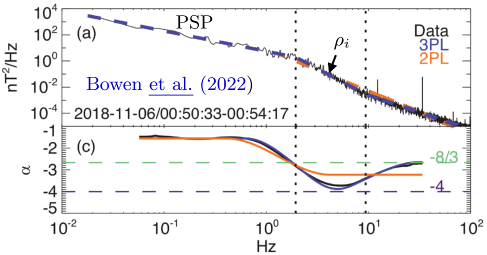

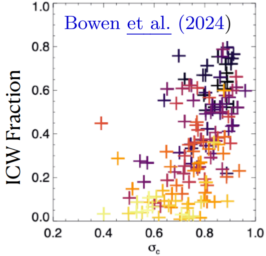

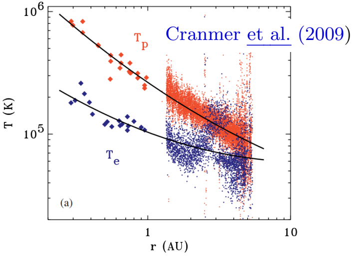

Helicity barrier "in situ"

- The (fast) solar wind generally has $\beta_e \gg \beta_e^{\rm crit}$, and so we would expect to see observational signatures of the helicity barrier.

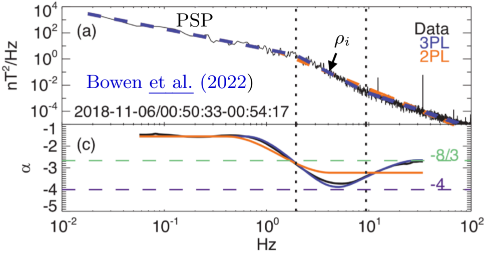

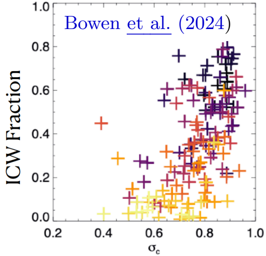

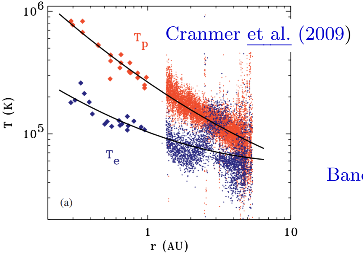

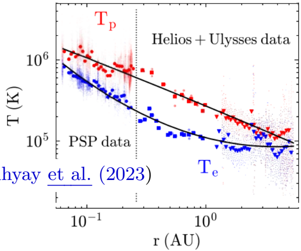

Summary

- In imbalanced isothermal KREHM, nonlinear conservation laws imply the existence of a critical electron beta

$$\boxed{\beta_e^{\mathrm{crit}} = \frac{2Z}{1+\tau/Z}\frac{m_e}{m_i}\frac{1}{\sigma_\varepsilon^2}.}$$

- A "switch" between two fundamentally different types of turbulence and resultant heating:

$\beta_e \lesssim \beta_e^{\mathrm{crit}}$,
constant flux,
$Q_e \gg Q_i$

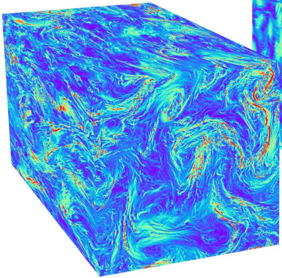

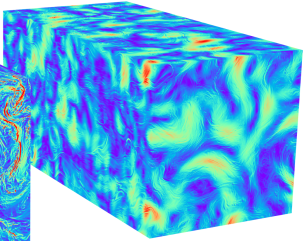

$\beta_e \gtrsim \beta_e^{\mathrm{crit}}$, **helicity barrier**,
$Q_e \ll Q_i$

- Recent work: re-introducing electron kinetics (Landau damping) $\Rightarrow$ appears to act as a linear damping on the energy

Summary

- In imbalanced isothermal KREHM, nonlinear conservation laws imply the existence of a critical electron beta

$$\boxed{\beta_e^{\mathrm{crit}} = \frac{2Z}{1+\tau/Z}\frac{m_e}{m_i}\frac{1}{\sigma_\varepsilon^2}.}$$

- A "switch" between two fundamentally different types of turbulence and resultant heating:

$\beta_e \lesssim \beta_e^{\mathrm{crit}}$,
constant flux,
$Q_e \gg Q_i$

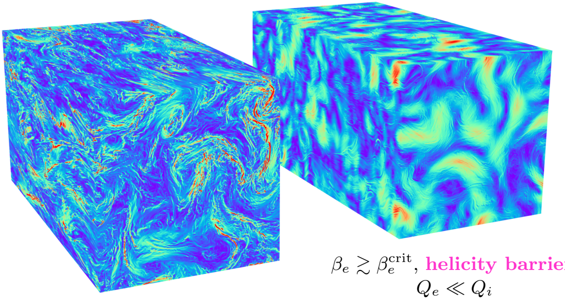

$\beta_e \gtrsim \beta_e^{\mathrm{crit}}$, **helicity barrier**,
$Q_e \ll Q_i$

arXiv

- Recent work: re-introducing electron kinetics (Landau damping) $\Rightarrow$ appears to act as a linear damping on the energy

Bandyopadhyay, R., Meyer, C. M., Matthaeus, W. H., McComas, D. J., Cranmer, S. R., Halekas, J. S., Huang, J., Larson, D. E., Livi, R., Rahmati, A., Whittlesey, P. L., Stevens, M. L., Kasper, J. C. & Bale, S. D. 2023 Estimates of proton and electron heating rates extended to the near-sun environment. *Astrophys. J. Lett.* **955**, L28.

Bowen, T.A., Bale, S. D., Chandran, B. D. G., Chasapis, A., Chen, C. H. K., Dudok de Wit, T., Mallet, A., Meyrand, R. & Squire, J. 2024 Mediation of collisionless turbulent dissipation through cyclotron resonance. *Nature Astron.* Doi: 10.1038/s41550-023-02186-4.

Bowen, T. A., Chandran, B. D. G., Squire, J., Bale, S. D., Duan, D., Klein, K. G., Larson, D., Mallet, A., McManus, M. D., Meyrand, R., Verniero, J. L. & Woodham, L. D. 2022 In situ signature of cyclotron resonant heating in the solar wind. *Phys. Rev. Lett.* **129**, 165101.

Chen, C. H. K. 2016 Recent progress in astrophysical plasma turbulence from solar wind observations. *J. Plasma Phys.* **82**, 535820602.

Chen, C. H. K., Boldyrev, S., Xia, Q. & Perez, J. C. 2013 Nature of subproton scale turbulence in the solar wind. *Phys. Rev. Lett.* **110**, 225002.

Cranmer, S. R., Matthaeus, W. H., Breech, B. A. & Kasper, J. C. 2009 Empirical constraints on proton and electron heating in the fast solar wind. *Astrophys. J.* **702**, 1604.

Kolmogorov, A. N. 1941 Local structure of turbulence in incompressible viscous fluid at very large Reynolds numbers. *Dokl. Acad. Nauk SSSR* **30**, 299.

Loureiro, N. F. & Boldyrev, S. 2018 Turbulence in magnetized pair plasmas. *Astrophys. J.* **866**, L14.

Meyrand, R., Squire, J., Schekochihin, A.A. & Dorland, W. 2021 On the violation of the zeroth law of turbulence in space plasmas. *J. Plasma Phys.* **87**, 535870301.

Milanese, L. M., Loureiro, N. F., Daschner, M. & Boldyrev, S. 2020 Dynamic Phase Alignment in Inertial Alfvén Turbulence. *Phys. Rev. Lett.* **125**, 265101.

Squire, J., Meyrand, R. & Kunz, M. W. 2023 Electron-Ion Heating Partition in Imbalanced Solar-wind Turbulence. *Astrophys. J. Lett.* **957**, L30.

Squire, J., Meyrand, R., Kunz, M. W., Arzamasskiy, L., Schekochihin, A. A. & Quataert, E. 2022 High-frequency heating of the solar wind triggered by low-frequency turbulence. *Nature Astron.* **6**, 715.